HGG Advances

REPORT

Biallelic pathogenic variants in the mitochondrial form of phosphoenolpyruvate carboxykinase cause peripheral neuropathy

Neal Sondheimer,[1,2,3,*] Alberto Aleman,[4] Jessie Cameron,[3] Hernan Gonorazky,[4] Nesrin Sabha,[2] Paula Oliveira,[2] Kimberly Amburgey,[4] Azizia Wahedi,[2] Dahai Wang,[2] Michael Shy,[5] and James J. Dowling.[1,2,4,6,*]

Summary

Phosphoenolpyruvate carboxykinase (PCK) plays a critical role in cytosolic gluconeogenesis, and defects in *PCK1* cause a fasting-aggravated metabolic disease with hypoglycemia and lactic acidosis. However, there are two genes encoding PCK, and the role of the mitochondrial resident PCK (encoded by *PCK2*) is unclear, since gluconeogenesis is cytosolic. We identified three patients in two families with biallelic variants in *PCK2*. One has compound heterozygous variants (p.Ser23Ter/p.Pro170Leu), and the other two (siblings) have homozygous p.Arg193Ter variation. All three patients have weakness and abnormal gait, an absence of PCK2 protein, and profound reduction in PCK2 activity in fibroblasts, but no obvious metabolic phenotype. Nerve conduction studies showed reduced conduction velocities with temporal dispersion and conduction block compatible with a demyelinating peripheral neuropathy. To validate the association between *PCK2* variants and clinical disease, we generated a mouse knockout model of *PCK2* deficiency. The animals present abnormal nerve conduction studies and peripheral nerve pathology, corroborating the human phenotype. In total, we conclude that biallelic variants in *PCK2* cause a neurogenetic disorder featuring abnormal gait and peripheral neuropathy.

Introduction

Phosphoenolpyruvate carboxykinase (PCK) plays a critical role in intermediary metabolism, converting the tricarboxylic acid cycle intermediate oxaloacetate into the gluconeogenic precursor phosphoenolpyruvate. There are two human genes encoding PCK. Cytosolic phosphoenolpyruvate carboxykinase (*PCK1*) encodes a protein with clear roles in hepatic gluconeogenesis, and loss-of-function variants cause a syndrome (MIM 261680) dominated by hypoglycemia during fasting.[1] Mitochondrial phosphoenolpyruvate carboxykinase (*PCK2*) encodes a protein with 70% identity to *PCK1* that is targeted to the mitochondrial matrix and expressed primarily in pancreas, kidney, liver, and fibroblasts.[2]

The cellular role of PCK2 is unclear, as gluconeogenesis is cytosolic. The mitochondrial PCK2 has kinetic properties similar to those of the cytosolic form and can substitute for PCK1 when targeted to the cytosol.[3] One hypothesis specific to its function in the mitochondrial matrix is that PCK2 is required for the consumption of mitochondrial guanosine triphosphate (GTP) and the regulation of pancreatic insulin secretion.[4] However, an animal model deficient in *Pck2*, while having impaired glucose-stimulated insulin secretion, was non-diabetic.[5]

While inherited defects in mitochondrial PCK2 were previously claimed in the medical literature (MIM 261650),[6,7] none of the patients described were known or found to have pathogenic variants in *PCK2*, making it unlikely that the disorder was correctly described.[8] In this study, we identify three individuals with biallelic *PCK2* variants and a phenotype consistent with an inherited neurogenetic condition featuring abnormal gait and peripheral neuropathy.

Results

Case presentations

Using exome sequencing, we identified three patients in two families with a common phenotype and likely pathogenic variants in *PCK2* (Figure 1A). Patient 1 came to medical attention as a 3-year-old girl with ataxia and weakness, which was exacerbated by illness. Specifically, she experienced several episodes of severe gait instability resulting in transient loss of ambulation and necessitating hospitalization. Between episodes she was found to have mild, persistent gait ataxia and mild distal > proximal weakness.

Owing to the episodic nature of the presentation, particularly given exacerbation with illness, an inborn error of metabolism was suspected and investigated. Mild elevations in lactate were occasionally noted (2.4–3.5 mM during her initial hospitalization) but metabolic studies were otherwise unremarkable, and a 24-h fasting study provoked a ketotic response (β-hydroxybutyrate 0.8 mM at 24 h).

[1]Departments of Paediatrics and Molecular Genetics, The University of Toronto, Toronto, ON, Canada; [2]Genetics and Genome Biology, The Hospital for Sick Children, Toronto, ON, Canada; [3]Divisions of Clinical and Metabolic Genetics, The Hospital for Sick Children, Toronto, ON, Canada; [4]Divisions of Neurology, The Hospital for Sick Children, Toronto, ON, Canada; [5]Department of Neurology, University of Iowa, Iowa City, IA, USA
[6]Lead contact
*Correspondence: neal.sondheimer@sickkids.ca (N.S.), james.dowling@sickkids.ca (J.J.D.)
https://doi.org/10.1016/j.xhgg.2023.100182.

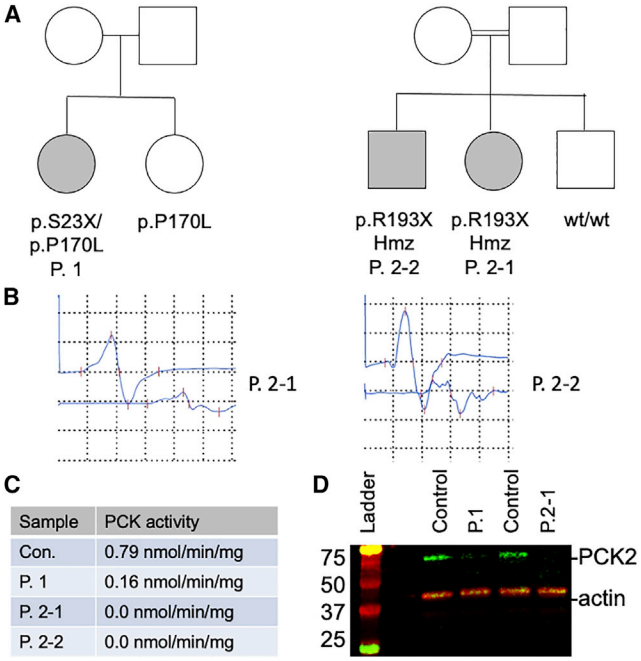

Sample	PCK activity
Con.	0.79 nmol/min/mg
P. 1	0.16 nmol/min/mg
P. 2-1	0.0 nmol/min/mg
P. 2-2	0.0 nmol/min/mg

Figure 1. *PCK2* variants are associated with peripheral neuropathy

(A) Pedigrees from two families with biallelic variants in *PCK2*.

(B) Nerve conduction studies (NCS) from right tibial nerve. In patient P.2-1, NCS showed low proximal and distal compound muscle action potential (CMAP) amplitudes (2.5 mV and 0.79 mV, respectively) with reduced conduction velocity (31.1 m/s) and temporal dispersion. In patient P.2-2, NCS showed low proximal and distal CMAP amplitudes (0.89 mV and 0.25 mV, respectively) with reduced conduction velocity (32.3 m/s) and temporal dispersion.

(C) Reduction in PCK2 activity in fibroblast lysates from patients harboring biallelic *PCK2* variants (Con., unrelated normal control).

(D) Western blot of fibroblast lysates from patients P.1 and P.2-1 and from two unrelated controls. Actin was provided as a loading control.

She was lost to follow-up for many years until she presented again in adulthood. She continues to experience gait ataxia but has maintained independent ambulation. No additional diagnostic data were able to be obtained; of note, nerve conduction studies have never been performed.

Whole-exome sequencing identified p.Ser23Ter (c.68C>G [NM004563.4]) and p.Pro170Leu (c.509C>T) variants in *PCK2* and no other potentially causative variants. An unaffected sibling carried the p.Pro170Leu variant only. The allele frequency of p.Ser23Ter is 1.87×10^{-3} and p.Pro170Leu is 4.78×10^{-5} in a database of large-scale sequencing projects (gnomAD v2.1.1, May 1, 2021 release).[9] The prevalence of p.Ser23Ter is unexpectedly high for a loss-of-function allele. Of note, a single p.Ser23Ter homozygous individual is found enumerated in GnomAD.

A second family was identified after referral of a 12-year old girl (patient 2-1) for abnormal gait. Her gait changes were progressive, with symptom onset at age 10 years and with increasing clumsiness and falls over an approximate span of 2 years. Family history revealed that her older brother (patient 2-2) was similarly affected and that the parents are first cousins. Physical examination of the proband was notable for distal muscle atrophy and bilateral pes cavus, distal muscle weakness, and absent reflexes in the knees and ankles. Sensory exam was abnormal in the lower extremities to all modalities. Of note, both the proband and her brother had evidence of asymmetry in terms of muscle atrophy and weakness. Unlike with individual 1, there was no clear demonstration of fluctuation in symptomatology or worsening with illness in either sibling.

Nerve conduction studies, performed on both siblings, showed a sensory-motor demyelinating peripheral neuropathy with evidence of temporal dispersion and conduction block (Figure 1B and Table S1). As with the physical exam, there were asymmetrical changes in nerve conduction. Metabolic studies, including lactate, pyruvate, amino acids, and urine organic acids, were unremarkable. The proband was initially diagnosed, based on the nerve conduction studies, with chronic inflammatory demyelinating polyneuropathy and treated with intravenous immunoglobulin. After failure of response to therapy, genetic testing was pursued. PMP22 deletion/duplication testing was normal, and a Charcot-Marie-Tooth disease multigene panel was unremarkable. Whole-exome sequencing identified homozygous p.Arg193Ter variants in *PCK2* in both siblings (c.577C>T [NM004563.4]), which had a population allele frequency of 8.14×10^{-5}. A third sibling in the family had normal gait and did not carry the variant. Of note, no other disease-associated pathogenic variants were identified in either sibling.

Validation studies: Patient fibroblasts show reduced PCK2 levels and activity

Fibroblast samples were obtained from all patients. Since *PCK1* is not expressed in fibroblasts,[2] enzymatic studies of PCK activity in these cells reflects *PCK2* alone. There was a partial loss of fibroblast PCK2 activity in fibroblasts from patient 1, and a complete loss of activity in cells from patients 2-1 and 2-2 (Figure 1C). Western blotting of fibroblast lysates confirmed a partial loss of detectable PCK2 in patient 1 and a complete loss of protein in patient 2-1 (Figure 1D). Oximetry studies of intact fibroblasts showed no significant difference in basal or maximal oxygen consumption between control cells and cells from patient 2-1 (Figure S1), consistent with a lack of defect in mitochondrial oxidative phosphorylation.

Characterization of a *Pck2* knockout mouse line

To further investigate the connection between the phenotype and *PCK2* variants, we created and evaluated a mouse model of *Pck2* deficiency (*Pck2_em1_del* or *Pck2* KO). This mouse line, generated on a C57BL/6NCrl background, harbors a homozygous 252 bp deletion in *Pck2*, resulting in a p.Ser142Hisfs*21 nonsense mutation (see supplemental material and methods for details of the generation of this strain). Homozygous animals were viable with no overt phenotype but were obtained at slightly below expected

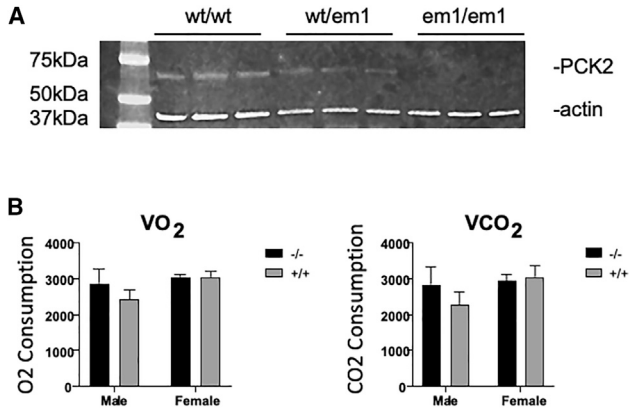

Figure 2. Characterization of mouse embryonic fibroblasts from *Pck2* knockout mice

(A) Western blotting of wild-type (wt), heterozygous (wt/em1), and *Pck2* knockout (em1/em1) animals. Actin was used as a control. Protein extracts were derived from mouse embryonic fibroblasts for the indicated genotypes.

(B) Metabolic studies of *Pck2* knockout compared with wild-type mice (n = 8 animals studied).

VO_2 p = 0.20 and VCO_2 p = 0.017 by two-way ANOVA without Bonferroni correction.

frequency (22%; 53/240), with a mild bias toward male survival (30% of males homozygous, 15% of females homozygous).

Murine embryonic fibroblast (MEF) lines were created from wild-type, heterozygous, and homozygous *Pck2* KO animals. Western blotting of the cell lines showed an absence of protein in the *Pck2* KO animals and a partial loss of protein in the heterozygotes (Figure 2A). Studies of PCK activity in lysates showed a corresponding loss of activity in *Pck2* KO MEFs compared with wild-type MEFs (wild type = 0.57 ± 0.04 nmol/min/mg protein, *Pck2* KO = 0.0 nmol/min/mg protein).

We performed a battery of phenotypic analyses on the *Pck2* KO animals, comparing them with wild-type littermates, with independent evaluation of both male and female animals because of the observed difference in viability. A small difference was seen in metabolic studies in the males, with increased volume of oxygen consumed (VO_2) and volume of CO_2 produced (VCO_2) in the KO animals that was no longer significant after correction for multiple testing (Figure 2B). Treadmill testing was used to evaluate the animal's gait. Minor differences were noted in gait, primarily in female animals, but these again were not significant after correction for multiple testing.

We then focused additional investigations on the peripheral nervous system. *Pck2* KO animals and wild-type littermates were evaluated by nerve conduction studies, where we observed in KO mice an asymmetric reduction of the conduction velocities (Figure 3A), mainly in males, associated with variable penetrance. Some of the KO mice also showed mild temporal dispersion, a finding not seen in any wild-type mice. Considering 40 m/s as the lower limit of normal for sural nerve conduction velocity, 6 of 15 *Pck2* KO mice had reduced values (i.e., <40 m/s) while only 1 of 15 wild-type littermates showed a reduction (Table S2). Lastly, we examined for peripheral nerve pathology using both light and electron microscopy. No obvious structural abnormalities were consistently observed. Quantitative analysis of sciatic nerves, however, revealed variability in both axon and myelin sheath diameter (Figure 3B), with significant shifts to disproportionate amounts of small or large fibers (Figures 3C and S2). In total, these findings support the presence in KO mice of a demyelinating peripheral neuropathy of variable penetrance.

Discussion

In summary, our studies demonstrate that the loss of *PCK2* causes a neurogenetic disorder featuring abnormal gait with evidence of demyelinating peripheral neuropathy. This phenotype stands in contrast to the decompensating metabolic condition that has been associated with the loss of *PCK1*. The difference in phenotype is likely related to the targeting of PCK to the mitochondrial matrix and its expression in a different set of tissues. There is no evidence of any diabetic phenotype in the patients or animal model, although there were small changes in mitochondrial coupling in the male *Pck2* KO animals.

Previous studies of *PCK2* posited a role in pancreatic insulin release. However, none of our patients are diabetic, and patient 1 had an unremarkable glucose tolerance test as a child. Although *PCK2* is apparently highly expressed in liver and pancreas,[2] we observed no deficits in our patients or in the KO mice corresponding to hepatic or endocrine or exocrine pancreatic function. We conclude that a loss of mitochondrial PCK activity is not diabetogenic.

The clinical phenotype, at least in family 2 and also supported by the mouse studies, is in keeping with a recessive form of Charcot-Marie-Tooth disease (CMT type 4) or hereditary motor and sensory neuropathy. A key unanswered question of this study concerns the mechanism through which the loss of mitochondrial PCK activity causes peripheral neuropathy. Previous studies have implicated *PCK2* in the maintenance of neuronal progenitor state in cell culture,[10] and loss of this function may explain the histopathological finding of excessive variability of axon diameter. However, it is unclear how this finding relates to the demyelination changes observed in our patients or to the temporal dispersion of nerve conduction signals seen in both patients and mice. From a pathomechanistic prospective, PCK2 deficiency fits with the broader subgroup of peripheral neuropathies due to abnormalities in mitochondrial structure and/or function, a group that includes mutations in *MFN2* (CMT2A), *SURF1* (CMT4K), and *PDK3* (CMTX6).

Of note, neither isoform of PCK is highly expressed in the central nervous system, although *PCK2* is detectable in many brain regions where *PCK1* expression is absent. A study of dogs with paroxysmal dyskinesia has recently implicated a heterozygous variant in the GTP-binding domain of *PCK2* as causative.[11] One possible avenue for

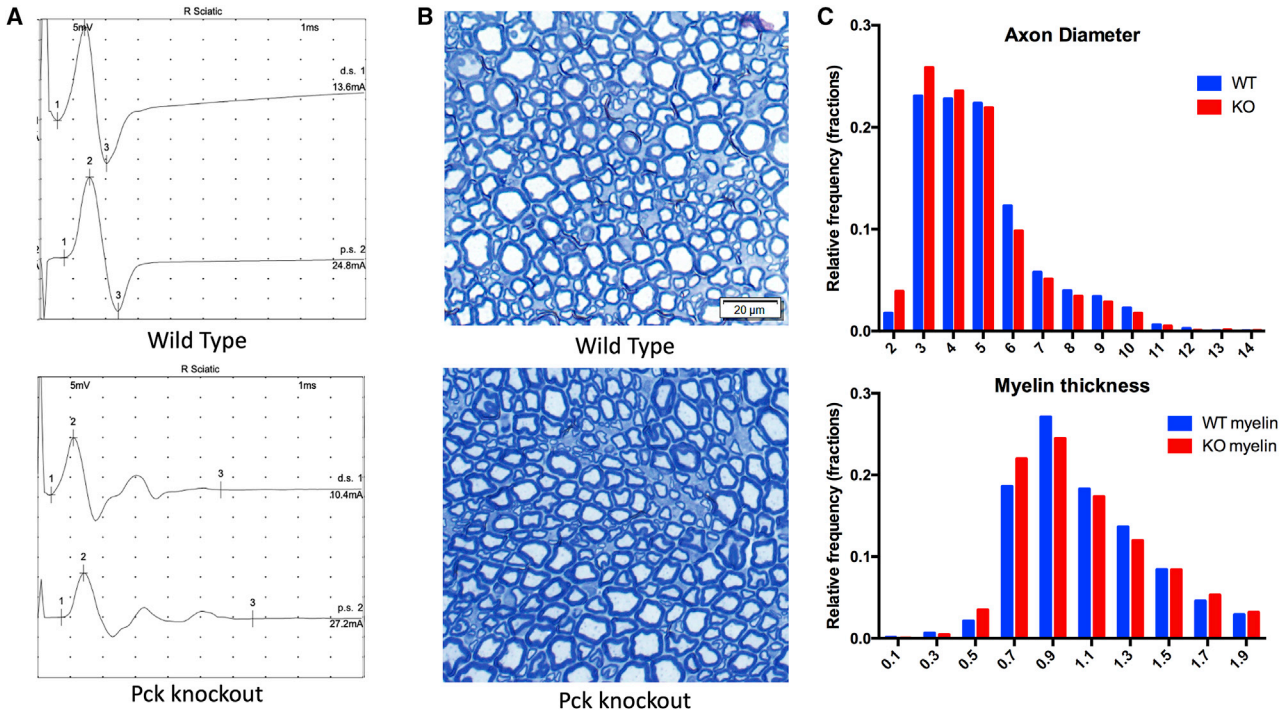

Figure 3. Peripheral nervous system changes in *Pck2* knockout mice

(A) Sciatic nerve conduction studies of *Pck2* knockout mice reveal reduced conduction velocities and temporal dispersion (Table S2) (n = 15 per genotype). Shown are representative tracings from a wild-type littermate and a *Pck2* knockout mouse.

(B) Representative semi-thin sections of sciatic nerve. No overt abnormalities were seen, although there was the appearance of an increased proportion of small fibers.

(C) Quantification of axon diameter and myelin thickness as represented by frequency distribution plots. Difference in distribution between genotypes was p = 0.0001 (Wilcoxon rank test, n = 8 per genotype with >50 fibers measured per nerve/animal).

future studies is investigating whether the clearance of GTP in the mitochondrial matrix by PCK may be important for the maintenance of neuronal health.

The phenotype described in our patients is relatively mild in that all three individuals have maintained the ability to ambulate independently. Given the relatively high allele frequency of loss-of-function variants in PCK2, particularly the p.Ser23Ter allele, combined with mild phenotypic presentations, we posit that deficiency in *PCK2* may be a fairly common genetic cause of peripheral neuropathy that is significantly underdiagnosed. As the sequencing of patients with ataxia, gait disturbance, and/or abnormal nerve conduction studies becomes more common, we suspect that *PCK2* variants will be increasingly recognized as a cause of human neurological disease.

Supplemental information

Supplemental information can be found online at https://doi.org/10.1016/j.xhgg.2023.100182.

Acknowledgments

We thank the patients and families for agreeing to participate in this study. This study was funded in part through a Rare Disease Models and Mechanisms grant from the Canadian Institutes of Health Research (N.S., M.S.). Additional support was provided by the Mogford Campbell Family endowed chair fund (J.J.D.). We thank the Toronto Center for Phenogenomics for assistance with the *Pck2* knockout mouse model.

Declaration of interests

N.S. is an employee of Synlogic, and K.A. is a part-time employee of Deep Genomics.

Received: July 22, 2022
Accepted: January 18, 2023

References

1. Vieira, P., Cameron, J., Rahikkala, E., Keski-Filppula, R., Zhang, L.H., Santra, S., Matthews, A., Myllynen, P., Nuutinen, M., Moilanen, J.S., et al. (2017). Novel homozygous PCK1 mutation causing cytosolic phosphoenolpyruvate carboxykinase deficiency presenting as childhood hypoglycemia, an abnormal pattern of urine metabolites and liver dysfunction. Mol. Genet. Metabol. *120*, 337–341.
2. Modaressi, S., Brechtel, K., Christ, B., and Jungermann, K. (1998). Human mitochondrial phosphoenolpyruvate carboxykinase 2 gene. Structure, chromosomal localization and tissue-specific expression. Biochem. J. *333*, 359–366.
3. Escós, M., Latorre, P., Hidalgo, J., Hurtado-Guerrero, R., Carrodeguas, J.A., and López-Buesa, P. (2016). Kinetic and functional properties of human mitochondrial phosphoenolpyruvate carboxykinase. Biochem. Biophys. Rep. *7*, 124–129.

4. Stark, R., Pasquel, F., Turcu, A., Pongratz, R.L., Roden, M., Cline, G.W., Shulman, G.I., and Kibbey, R.G. (2009). Phosphoenolpyruvate cycling via mitochondrial phosphoenolpyruvate carboxykinase links anaplerosis and mitochondrial GTP with insulin secretion. J. Biol. Chem. *284*, 26578–26590.
5. Abulizi, A., Cardone, R.L., Stark, R., Lewandowski, S.L., Zhao, X., Hillion, J., Ma, L., Sehgal, R., Alves, T.C., Thomas, C., et al. (2020). Multi-Tissue acceleration of the mitochondrial phosphoenolpyruvate cycle improves whole-body metabolic health. Cell Metabol. *32*, 751–766.e11.
6. Robinson, B.H., Taylor, J., and Sherwood, W.G. (1980). The genetic heterogeneity of lactic acidosis: occurrence of recognizable inborn errors of metabolism in pediatric population with lactic acidosis. Pediatr. Res. *14*, 956–962.
7. Clayton, P.T., Hyland, K., Brand, M., and Leonard, J.V. (1986). Mitochondrial phosphoenolpyruvate carboxykinase deficiency. Eur. J. Pediatr. *145*, 46–50.
8. Bodnar, A.G., Cooper, J.M., Holt, I.J., Leonard, J.V., and Schapira, A.H. (1993). Nuclear complementation restores mtDNA levels in cultured cells from a patient with mtDNA depletion. Am. J. Hum. Genet. *53*, 663–669.
9. Karczewski, K.J., Francioli, L.C., Tiao, G., Cummings, B.B., Alföldi, J., Wang, Q., Collins, R.L., Laricchia, K.M., Ganna, A., Birnbaum, D.P., et al. (2020). The mutational constraint spectrum quantified from variation in 141,456 humans. Nature *581*, 434–443.
10. Álvarez, Z., Hyroššová, P., Perales, J.C., and Alcántara, S. (2016). Neuronal progenitor maintenance requires lactate metabolism and PEPCK-M-directed cataplerosis. Cerebr. Cortex *26*, 1046–1058.
11. Nessler, J., Hug, P., Mandigers, P.J.J., Leegwater, P.A.J., Jagannathan, V., Das, A.M., Rosati, M., Matiasek, K., Sewell, A.C., Kornberg, M., et al. (2020). Mitochondrial PCK2 missense variant in shetland sheepdogs with paroxysmal exercise-induced dyskinesia (PED). Genes *11*, 774–815.

HGGA, Volume *4*

Supplemental information

Biallelic pathogenic variants in the mitochondrial form of phosphoenolpyruvate carboxykinase cause peripheral neuropathy

Neal Sondheimer, Alberto Aleman, Jessie Cameron, Hernan Gonorazky, Nesrin Sabha, Paula Oliveira, Kimberly Amburgey, Azizia Wahedi, Dahai Wang, Michael Shy, and James J. Dowling.

Supplement

Supplemental material and methods

Patient information

Written informed consent was obtained from all study participants via an REB approved protocol (Dowling REB#: 1000009004, Hospital for Sick Children, REB#: 1000009004). Commercial whole exome sequencing was performed at GeneDx. Nerve conduction studies were performed as part of routine clinical care (Gonorazky, Hospital for Sick Children).

Patient variants
Subject P.1 has PCK2 variants c.68C>G; p.S23X (ClinVar ID 374449) and c.509C>T; p.P170L (ClinVar ID pending). Subjects P. 2-1 and P. 20-2 are homozygous for the PCK2 variant c.577C>T; p.R193X (ClinVar ID 451808).

Patient fibroblast studies

Fibroblasts were obtained from the palmar surface of the distal upper extremity. Local anesthetic was used for pain control. Cultures were established at the diagnostic resource centre (Hospital for Sick Children), and then experiments were performed on early passage cells.

Mouse line details

The mouse line C57BL/6N-Pck2<em1(IMPC)Tcp>/Tcp was made as part of the KOMP2-Phase2 project (https://www.mousephenotype.org/) and generated at The Centre for Phenogenomics . It was obtained from the Canadian Mouse Mutant Repository.

Mouse nerve conduction studies

Nerve conduction studies were performed as per Schulz et al (2014) with minor modifications. Mice were anesthetised with 3% isoflurane/100% oxygen by inhalation for initiation of anesthesia and then maintained on 2% isoflurane/100% oxygen for the procedure. For stimulation and recording, we used a portable electromyography unit (Nicolet VikingQuest System, WI USA) and subdermal needle electrodes of 13 mm length. Compound muscle action potentials were recorded from the gastrocnemius muscle after stimulation of the sciatic nerve (see Supplemental Figure 3).

Mouse nerve pathology assessment

Sciatic nerves from knockout (n = 8) and wild type (n = 6) animals were dissected and immediately place at 4°C in EM fixative (4% paraformaldehyde, 2% glutaraldehyde containing 0.1 M sodium cacodylate buffer). Samples were incubated overnight, then taken to the Advanced Bioimaging Center (The Hospital for Sick Children), where they

were dehydrated and then embedded for sectioning. Semi-thins sections were cut and stained with toluidine blue. Micrographs were captured with an Infinity1 camera (Lumenera Corporation, Ottawa, CA) with CellSens Standard software visualized through an Olympus BX43 light microscope (Olympus, Center Valley, PA). Three different fields per slide were photographed, using 200x magnification.

For quantification, images were prepared using ImageJ Fiji software (Rasband, 1997-2018), starting with setting the scale and transforming the image to 8-bit. They were then segmented using AxonSeg (Zaimi A, 2016). Using this software, we first determined manually the pixel size, the threshold of axon segmentation, and axon discrimination parameters (minimal size, solidity and ellipticity). The same parameters were used on all images. Checking of segmentation was done after processing, and segments were removed or added manually. After setting the parameters, relevant morphometric data were automatically extracted, with the software calculating myelin thickness, myelin area, axon area, and axon diameter, and then generating a table with all data that can be opened using Matlab (Natick, 2021).

Using Excel (Microsoft Corporation, 2018. Microsoft Excel), the data obtained from the 3 fields was added to calculate average axon diameter distribution, axon density and the myelin thickness distribution. Analyses of each parameter in order to evaluate statistical significance were made using GraphPad Prism version 9.1.2 for Windows (GraphPad Software, San Diego, California USA, www.graphpad.com).

References

Natick, M. T. (2021). MATLAB. version R2021a.

Schulz, A., Walther, C., Morrison, H., Bauer, R (2014). In Vivo Electrophysiological Measurements on Mouse Sciatic Nerves. J. Vis. Exp. (86), e51181.

Rasband, W. (1997-2018). ImageJ. *National Institutes of Health, Bethesda, Maryland, USA*. Retrieved from https://imagej.nih.gov/ij

Zaimi A, D. T.-A. (2016). AxonSeg: Open Source Software for Axon and Myelin Segmentation and Morphometric Analysis. *Front Neuroinform*, 10:37. doi:10.3389/fninf.2016.00037

Supplemental figures and tables

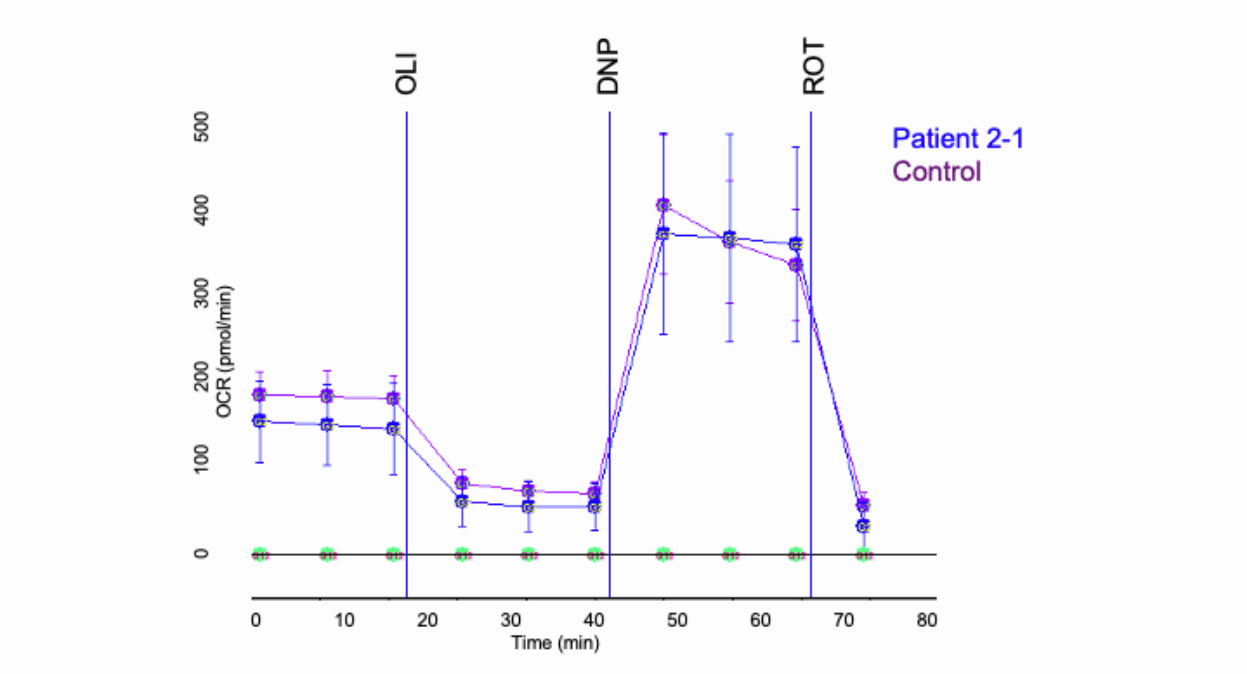

Figure S1 Oximetry of patient fibroblasts
Oximetry studies were performed using intact fibroblasts from P. 2-1 and an unrelated control. Oligomycin (OLI), dinitrophenol (DNP) and rotenone/antimycin A (ROT) were added at the indicated times. Analysis, quantitation and statistics were performed on an XF-96 oximeter (Seahorse). There were no significant differences at any time point.

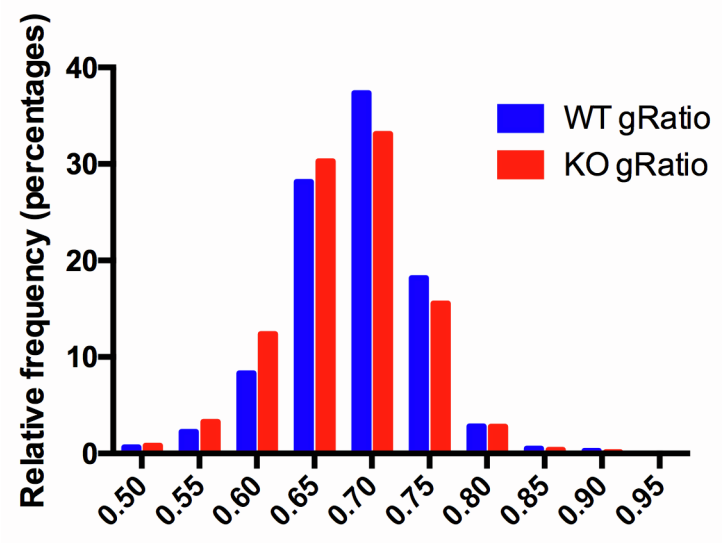

Figure S2: Abnormal g ratios in *Pck2* knockout sciatic nerves.
Sciatic nerves were dissected, processed, cut as semi thin sections, and then evaluated under light microscopy. Axon diameter, myelin sheath diameter, and the inner-to-outer sheath distance were all obtained. G ratios were calculated for all nerves. The g ratio (r/R) is the ratio between the inner and outer diameters of the myelin sheath, and is computed from the axon volume fraction (r) and the nerve (axon + myelin) volume fraction (R). G ratios were shifted to the left in knockout nerves, representing thinner myelin sheaths per axon diameter. ($p = 0.00001$).

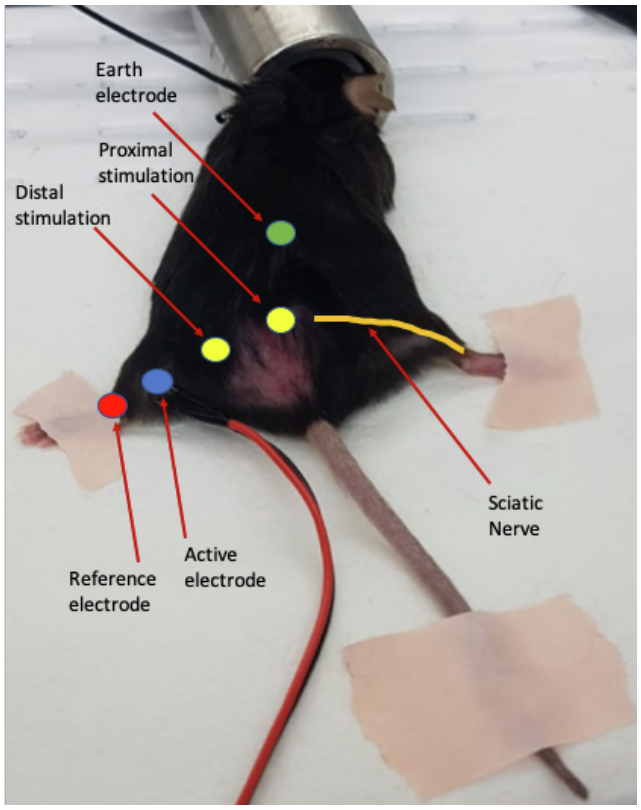

Figure S3: Sciatic motor nerve conduction velocity (NCVs) analyses. Measurement of electrophysiological responses of the sciatic nerve *in vivo* with the different positions of the electrodes used (adapted with minor changes from Schulz et al, 2014). Recording was done over gastrocnemius muscle (blue), with additional electrodes at reference (red) and ground/earth (green) sites. Stimulation was performed using needle electrodes at defined positions for proximal and distal stimulation sites (yellow). The orange line shows the approximate location of the sciatic nerve.

Table S1

A. Patient 1.1

Nerve stimulated	Site stimulation	Distal latency (m/s)	Amplitude (Motor=mV - Sensory=uV)	Conduction velocity (m/s)	F-wave Latency ms
L median (S)	Wrist	NR			
R ulnar (S)	Wrist	NR			
L superficial peroneal (S)	Leg	1.79	11.2	39.1	
R sural (S)	Calf	NR			
	Wrist	3.58	5.2		
R median (M)	Elbow	8.79	3.2	46.1	
	Wrist	3.16	4.1		
L ulnar (M)	Ab elb	9.56	4.8	37.5	
	Ankle	3.87	1.55		
R peroneal	Ab knee	13.8	0.76	34.2	
	Ankle	4.55	1.17		
L peroneal	Ab knee	13.0	0.39	36.5	
	Ankle	5.79	3.6		
L tibial	Knee	15.8	2.6	38.0	61.5
	Ankle	3.93	2.5		
R tibial	Knee	15.4	0.79	31.1	

B. Patient 1.2

Nerve stimulated	Site stimulation	Distal latency (m/s)	Amplitude (Motor=mV - Sensory=uV)	Conduction velocity (m/s)	F-wave Latency ms
L median (S)	Wrist	2.04	23,0	49.0	
L ulnar (S)	Wrist	1.50	12.1	50.0	
L superficial peroneal (S)	Leg	NR			
R sural (S)	Calf	NR			
	Wrist	3.77	4.7		
L median (M)	Elbow	10.2	4.2	38.9	
	Wrist	4.01	5.1		
L ulnar (M)	Ab elb	10.7	3.0	38.8	
	Ankle	6.70	0.80	28.9	
L tibial	Knee	20.2	0.42		NR
	Ankle	6.08	1.31		
R tibial	Knee	20.4	0.54	30.7	

N: No Response; R: right; L: left; S: sensory; M: motor.

Table S1. Nerve conduction studies from PCK2 patients.
Nerve conduction studies from two siblings with biallelic *PCK2* pathogenic variation. In both cases, the nerve conduction study showed primarily sensory-motor demyelinating length-dependent polyneuropathy. There was also evidence of temporal dispersion in some nerves, as well as important asymmetry in velocities and amplitudes.

	Genotype	Gender	Sciatic nerve (side)	Distal CMPA amplitude (mV)	Proximal CMPA amplitude (mV)	Temporal dispersion	Conduction velocity (m/s)
			R	37,5	29,8		40,0
1	KO	M	L	14,5	12,5		47,1
			R	27,4	26,6		58,7
2	KO	M	L	22,2	23,0		52,9
			R	44,7	58,7		58,0
3	KO	M	L	67,6	61,3		64,7
			R	16,6	14,0		16,0
4	KO	M	L	16,7	30,5		38,0
			R	17,9	21,4		32,0
5	KO	F	L	22,1	24,1		26,0
			R	25,0	20,4		36,0
6	KO	M	L	5,1	4,6	Present	37,0
			R	9,7	10,5		62,0
7	KO	M	L	23,1	21,7		96,0
			R	14,2	11,5		54,0
8	KO	M	L	7,7	7,7		58,0
			L	18,1	20,5		61,0
9	KO	F	R	11,2	21,2		72,0
			L	29,9	29,4		41,0
10	KO	F	R	24,7	26,3		38,0
			L	19,8	11,5		33,0
11	KO	F	R	9,7	14,9		36,0
			L	18,5	26,6		83,0
12	KO	F	R	25,0	27,0		36,0
			R	18,3	15,2		82,0
13	KO	F	L	24,1	29,4		96,0
			R	22,6	21,8		62,0
14	KO	F	L	17,0	21,0		67,0
			R	15,3	15,6	Present	35,0
15	KO	F	L	24,9	28,5		42,0
			R	23,4	20,3		62,0
16	WT	F	L	18,3	22,9		72,0
			R	47,3	49,9		58,8
17	WT	M	L	34,3	24,3		56,3
			R	7,9	8,0		64,0
18	WT	M	L	16,0	30,0		38,0
			R	12,8	21,1		32,0
19	WT	F	L	24,5	22,5		34,0
			R	16,1	18,0		70,0
20	WT	F	L	19,3	18,8		35,0
			R	7,1	7,5		91,0
21	WT	M	L	11,1	10,6		105,0
			R	15,6	15,6		87,0
22	WT	M	L	18,5	23,3		104,0
			R	34,3	33,8		82,0
23	WT	M	L	22,3	21,1		47,0
			R	15,3	13,4		67,0
24	WT	M	L	14,0	11,1		38,0
			L	16,7	28,9		83,0
25	WT	F	R	22,7	26,1		65,0
			R	12,3	14,0		41,0
26	WT	F	L	13,5	11,8		41,0
			R	19,4	18,5		62,0
27	WT	F	L	40,7	43,1		67,0
			R	18,9	17,7		46,0
28	WT	F	L	13,4	14,3		48,0
			R	15,6	25,2		83,0
29	WT	F	L	11,9	17,3		83,0
			R	20,0	24,9		53,0
30	WT	F	L	10,1	8,9		53,0

KO: Knockout; WT: wilde type; M: male; F: female; R: right; L: left.

Table S2. Mouse sciatic nerve motor conduction values.

Individual compound muscle action potential (CMAP) amplitudes and sciatic nerve conduction velocities for all mice in the study (n = 15 per group, *Pck2* knockout = KO and wild type = WT). Note that temporal dispersion, a sign of demyelination, was only seen in

KO mice. Additionally, 6/15 KO mice had reduced conduction velocities (defined as velocity < 40 m/s), while only 1/15 WT had reduced velocities.